J. Phys. B: At. Mol. Opt. Phys. **28** (1995) 1821–1833. Printed in the UK

Electron capture and transfer ionization in collisions of fast H^+ and He^{2+} ions with Cu atoms

M B Shah, C J Patton, M A Bolorizadeh†, J Geddes and H B Gilbody
Department of Pure and Applied Physics, The Queen's University of Belfast, Belfast, UK

Received 28 November 1994, in final form 16 January 1995

Abstract. One-electron capture involving either simple charge transfer or transfer ionization leading to the formation of Cu^{q+} ions for $q = 1$–5 has been studied for H^+–Cu collisions in the energy range 70–720 keV amu^{-1}. Both one- and two-electron capture by He^{2+} ions leading to Cu^{q+} ions for $q = 1$–7 and $q = 2$–5 in the ranges 35–360 keV amu^{-1} and 35–150 keV amu^{-1} respectively have been determined. A crossed beam coincidence counting technique has been used to measure cross sections for each of these processes corresponding to particular values of q. In the case of H^+–Cu collisions, measured fractions of Cu^{q+} ions formed in particular states of q have also been satisfactorily described in terms of an independent electron model with electron removal from either the 4s or 3d subshells. Comparisons between the present cross sections for H^+ and He^{2+} impact have also been made with the corresponding values previously measured for iron.

1. Introduction

Experimental studies of the multiple ionization of various atomic targets by ion impact have been quite extensive. However, the use of coincidence counting techniques to identify the contributions of specific collision mechanisms unambiguously has been most useful (see reviews by Salzborn and Müller (1986) and Cocke and Olson (1991)). To date, studies of multiple ionization of metallic atoms by ion impact have been very limited in spite of the fact that a detailed understanding of collision processes involving many stages of ionization of such species is important in astrophysics and in the physics of controlled thermonuclear fusion plasmas.

In recent work in this laboratory (Patton *et al* 1994), we studied the multiple ionization of iron atoms by 70–500 keV amu^{-1} H^+ and 37.5–360 keV amu^{-1} He^{2+} ions using a crossed beam coincidence counting technique. At the energies considered, the multiply charged Fe^{q+} ions observed (for up to $q = 6$) arise predominantly through transfer ionization (i.e. electron capture simultaneous with ionization). Measured cross sections were considered in terms of a model involving electron capture of either 4s, 3d or 3p electrons together with electron removal through binary collisions at high velocities.

In the present work we have used a similar experimental approach to study the formation of Cu^{q+} ions for q between 1 and 5 in collisions of 70–720 keV amu^{-1} H^+ ions and for q between 1 and 7 in collisions of 35–360 keV amu^{-1} He^{2+} with copper atoms. Unlike Fe, Cu has a completely filled 3d subshell and a single 4s electron. Cross sections ${}_{10}\sigma_{0q}$ for one-electron capture by H^+ ions

$$H^+ + Cu \rightarrow H + Cu^{q+} + (q-1)e \tag{1}$$

† Permanent address: Department of Physics, Shahid Bahonar University, Kerman, Iran.

0953-4075/95/091821+13$19.50

for $q = 1$–5 have been determined. Here $q = 1$ corresponds to simple charge transfer while $q > 1$ corresponds to transfer ionization. In addition, the measured charge state fractions F_q of the slow Cu^{q+} products have been considered in terms of an independent electron ionization model of ionization of the 4s and 3d electrons.

In the case of He^{2+} impact cross sections ${}_{20}\sigma_{1q}$ for the one-electron capture processes

$$He^{2+} + Cu \rightarrow He^{+} + Cu^{q+} + (q-1)e \tag{2}$$

for $q = 1$–7 have been determined. In addition cross sections ${}_{20}\sigma_{0q}$ for the two-electron capture processes

$$He^{2+} + Cu \rightarrow He + Cu^{q+} + (q-2)e \tag{3}$$

have been determined for $q = 2$–5.

2. Experimental approach

2.1. General description

The basic experimental arrangement was similar to that used in our recent studies of Fe (Patton *et al* 1994) which in turn was developed from our earlier experiments (Shah and Gilbody 1981, 1982, Shah *et al* 1992). Only the main features need to be outlined here.

A momentum analysed beam of H^+ or He^{2+} ions of the required energy was arranged to intersect at 90° a thermal energy beam of Cu atoms in the ground state. The crossed beam region was maintained at a pressure of about 5×10^{-8} Torr. A description of the special oven source used to provide the Cu atom beam has been given previously (Shah *et al* 1993). At the normal operating temperature of 1700 °C, the Cu atom density in the crossed beam region was estimated to be $\cong 10^{10}$ atoms cm^{-3}.

The slow Cu^{q+} collision products were extracted from the crossed beam region by a transverse electric field (applied between two high transparency grids), accelerated through a potential difference of about 4 kV and counted by a particle multiplier with an efficiency essentially independent of q for $q > 1$ (cf Shah and Gilbody 1985). Cu^{q+} ions, in particular charge states q, could be identified and distinguished from signals due to background gas collision products by their different times of flight to the counter in accordance with their charge to mass ratios.

The primary ion beam was charge analysed by electrostatic deflection beyond the beam intersection region and a particle multiplier was used to count the fast selected products from (1), (2) or (3) in coincidence with the slow Cu^{q+} ions of specified q arising from the same collision events. A typical fast H/slow Cu^{q+} ion time-of-flight coincidence spectrum is shown in figure 1. The separate peaks corresponding to the yields of Cu^{q+} for $q = 1$–5 can be seen to be well resolved.

2.2. Measuring, calibration and normalization procedure

The cross section ${}_{10}\sigma_{0q}$ for an electron capture process (1) in which q is specified may be expressed as

$${}_{10}\sigma_{0q} = S(Cu^{q+})/k(Cu^{q+})k(H)\mu. \tag{4}$$

In this expression $S(Cu^{q+})$ is the measured fast H/slow ion coincidence signal per unit primary beam intensity; $k(Cu^{q+})$ is the detection efficiency of the slow Cu^{q+} products;

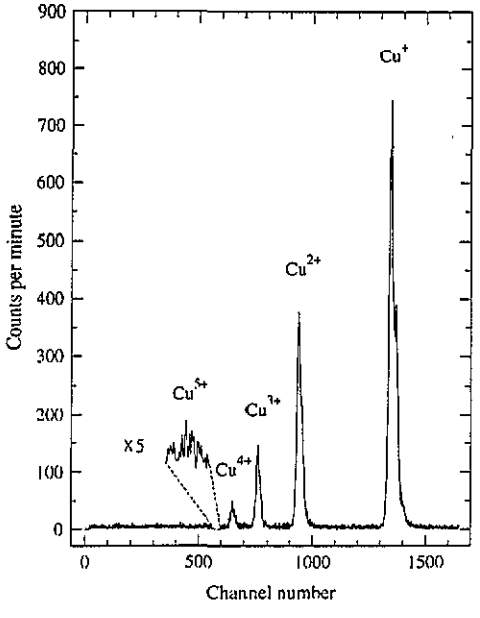

Figure 1. Fast H/slow Cu^{q+} ion coincidence time of flight spectrum showing Cu^{q+} products resulting from processes involving one-electron capture in collisions of 216 keV H^+ with copper atoms. Adjacent channels have a time separation of 2 ns.

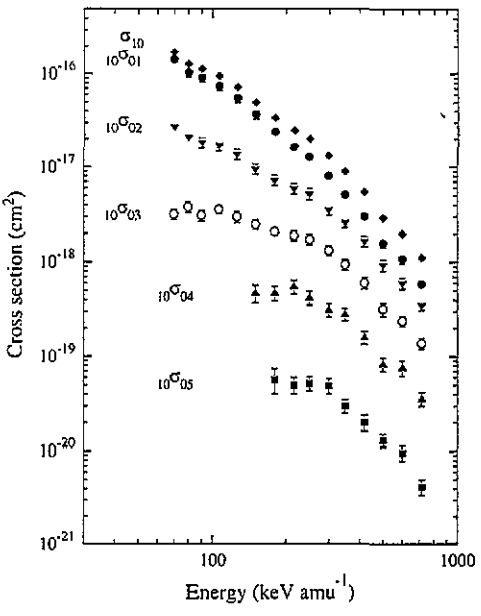

Figure 2. Cross sections ${}_{10}\sigma_{0q}$ for one-electron capture in collisions of H^+ with Cu atoms leading to Cu^{q+} products. Total one-electron capture cross sections σ_{10} are also shown.

k(H) is the detection efficiency (shown to be unity in the manner described previously) of the fast H atoms formed by electron capture; μ is the effective target thickness presented by the Cu atoms in the beam.

Our measured relative cross sections ${}_{10}\sigma_{0q}$ were normalized by reference to our recently measured cross sections σ_q(e) (Bolorizadeh *et al* 1994) for Cu^{q+} production by electron impact

$$e + Cu \rightarrow e + Cu^{q+} + qe. \tag{5}$$

The normalization procedure has been described in our previous work (Shah *et al* 1992). By means of a sliding mount, a pulsed electron gun was used to substitute an electron beam for the H^+ beam in precisely the same position with the Cu target conditions unchanged. The electron beam was pulsed with a repetition rate of 10^5 pulses s^{-1} and pulse duration of 200 ns. Immediately after the transit of an electron pulse through the target beam, slow Cu^{q+} ions formed in the crossed beam region were extracted by applying a delayed pulsed electric field across the high transparency grids in the manner described previously (Shah *et al* 1987).

The cross section σ_q(e) for Cu^{q+} production by electron impact may be expressed as

$$\sigma_q(e) = S_e(Cu^{q+})/k(Cu^{q+})\mu \tag{6}$$

where $S_e(Cu^{q+})$ is the yield of Cu^{q+} ions per unit electron beam intensity. Using an electron beam energy of 200 eV and our previous values of σ_1(e) and σ_2(e) due to Bolorizadeh *et al* (1994) (which in turn were normalized to absolute measurements of Freund *et al*

(1990) obtained using a fast intersecting beam technique) we obtained values of $k(Cu^+)\mu$ and $k(Cu^{2+})\mu$ in equation (6). In separate measurements we showed that $k(Cu^{q+})\mu$ for $q = 2$–5 was independent of q to within our measuring accuracy of 6%. These values of $k(Cu^{q+})\mu$ could then be used in equation (4) to obtain values of ${}_{10}\sigma_{0q}$ for specific transfer ionization processes. These same values could also be used in a similar way to obtain the corresponding values ${}_{20}\sigma_{1q}$ and ${}_{20}\sigma_{0q}$ for He^{2+} impact.

Throughout the measurements, as in our previous work with Fe, it was important to have a reliable continuous indication of the intensity of the Cu atom beam. A pulsed electron beam from a simple electron gun operating at 22 eV was arranged to intercept the Cu atom beam at a point beyond the main crossed beam region. The Cu^+ products were selectively identified by time-of-flight spectroscopy and recorded by a channeltron. This signal was used to monitor any changes in the Cu atom beam flux. The operation of the oven atom beam source with copper was found to be (inexplicably) less stable than with iron and measurements were therefore subject to greater uncertainties in reproducibility.

Table 1. Cross sections ${}_{10}\sigma_{0q}$ for one-electron capture in collisions of H^+ ions with Cu atoms leading to Cu^{q+} ions for $q = 1$–5. The total electron capture cross section σ_{10} is also shown. In addition to the uncertainties shown with individual cross sections, all values are subject to an estimated uncertainty of ±12% in absolute magnitude.

Energy (keV amu^{-1})	${}_{10}\sigma_{01}$ (10^{-17} cm^{-2})	${}_{10}\sigma_{02}$ (10^{-17} cm^2)	${}_{10}\sigma_{03}$ (10^{-18} cm^2)	${}_{10}\sigma_{04}$ (10^{-19} cm^2)	${}_{10}\sigma_{05}$ (10^{-20} cm^2)	σ_{10} (10^{-16} cm^2)
70	14.3 ± 1.3	2.7 ± 0.2	3.2 ± 0.4	—	—	1.73 ± 0.13
80	10.3 ± 1.1	2.1 ± 0.2	3.8 ± 0.5	—	—	1.28 ± 0.11
90	9.1 ± 1.0	1.83 ± 0.2	3.1 ± 0.4	—	—	1.12 ± 0.10
106	7.4 ± 0.8	1.70 ± 0.2	3.6 ± 0.4	—	—	0.95 ± 0.08
126	5.5 ± 0.6	1.37 ± 0.2	3.0 ± 0.4	—	—	0.72 ± 0.06
150	3.7 ± 0.4	0.95 ± 0.12	2.5 ± 0.3	4.7 ± 1.0	—	0.49 ± 0.04
180	2.4 ± 0.2	0.72 ± 0.09	2.1 ± 0.2	4.7 ± 0.8	5.7 ± 1.7	0.34 ± 0.022
216	1.64 ± 0.17	0.59 ± 0.07	1.91 ± 0.23	5.5 ± 0.9	5.0 ± 1.0	0.25 ± 0.019
250	1.28 ± 0.13	0.52 ± 0.07	1.75 ± 0.22	4.2 ± 0.7	5.2 ± 0.9	0.20 ± 0.015
300	0.80 ± 0.08	0.35 ± 0.04	1.32 ± 0.16	3.1 ± 0.5	4.9 ± 0.9	0.13 ± 0.009
350	0.51 ± 0.05	0.26 ± 0.03	0.94 ± 0.12	2.8 ± 0.4	3.0 ± 0.5	0.090 ± 0.006
420	0.30 ± 0.03	0.165 ± 0.021	0.60 ± 0.08	1.59 ± 0.25	2.0 ± 0.4	0.054 ± 0.004
500	0.159 ± 0.017	0.093 ± 0.012	0.32 ± 0.05	0.83 ± 0.13	1.3 ± 0.2	0.029 ± 0.002
600	0.108 ± 0.012	0.060 ± 0.008	0.24 ± 0.03	0.76 ± 0.14	0.96 ± 0.17	0.020 ± 0.001
720	0.059 ± 0.006	0.035 ± 0.004	0.14 ± 0.019	0.36 ± 0.06	0.42 ± 0.08	0.011 ± 0.001

3. Results and discussion

Table 1 lists our measured cross sections ${}_{10}\sigma_{0q}$ for one-electron capture by H^+ ions leading to Cu^{q+} ions in states $q = 1$–5 for impact energies in the range 70–720 keV amu^{-1}. The total one-electron capture cross section

$$\sigma_{10} \cong \sum_{q=1}^{q=5} {}_{10}\sigma_{0q}$$

is also listed.

Table 2. Cross sections $_{20}\sigma_{1q}$ for one-electron capture in collisions of He^{2+} ions with Cu atoms leading to Cu^{q+} ions for $q = 1$–7. The total one-electron capture cross section σ_{21} is also shown. In addition to the uncertainties shown with individual cross sections, all values are subject to an estimated uncertainty of ±12% in absolute magnitude.

Energy (keV amu^{-1})	$_{20}\sigma_{11}$ (10^{-16} cm^2)	$_{20}\sigma_{12}$ (10^{-16} cm^2)	$_{20}\sigma_{13}$ (10^{-16} cm^2)	$_{20}\sigma_{14}$ (10^{-16} cm^2)	$_{20}\sigma_{15}$ (10^{-17} cm^2)	$_{20}\sigma_{16}$ (10^{-18} cm^2)	$_{20}\sigma_{17}$ (10^{-18} cm^2)	σ_{21} (10^{-16} cm^2)
35	15.6 ± 1.3	5.2 ± 0.5	1.71 ± 0.20	0.39 ± 0.07	0.5 ± 0.2	—	—	23.0 ± 1.4
40	10.8 ± 0.9	4.5 ± 0.4	1.57 ± 0.19	0.40 ± 0.07	0.7 ± 0.2	1.1 ± 0.4	—	17.4 ± 1.0
46.5	9.0 ± 1.0	4.5 ± 0.5	1.66 ± 0.18	0.49 ± 0.09	1.0 ± 0.2	0.7 ± 0.4	—	15.8 ± 1.1
54	5.2 ± 0.6	3.1 ± 0.4	1.36 ± 0.16	0.39 ± 0.06	0.6 ± 0.2	—	—	10.1 ± 0.7
62.5	4.2 ± 0.5	2.7 ± 0.3	1.15 ± 0.13	0.41 ± 0.07	1.2 ± 0.2	1.8 ± 0.5	—	8.60 ± 0.6
75	2.9 ± 0.3	2.0 ± 0.2	0.89 ± 0.11	0.41 ± 0.06	1.3 ± 0.2	1.6 ± 0.5	—	6.35 ± 0.4
87.5	2.2 ± 0.3	1.65 ± 0.18	0.76 ± 0.09	0.36 ± 0.06	1.4 ± 0.2	1.5 ± 0.5	—	5.13 ± 0.4
105	1.47 ± 0.16	1.35 ± 0.16	0.72 ± 0.09	0.37 ± 0.06	1.2 ± 0.2	2.6 ± 0.5	—	4.06 ± 0.3
125	1.05 ± 0.12	0.89 ± 0.10	0.56 ± 0.07	0.29 ± 0.05	1.0 ± 0.2	2.0 ± 0.4	—	2.91 ± 0.2
150	0.88 ± 0.11	0.78 ± 0.09	0.48 ± 0.05	0.29 ± 0.05	1.2 ± 0.2	2.4 ± 0.5	—	2.57 ± 0.2
180	0.67 ± 0.08	0.57 ± 0.07	0.37 ± 0.05	0.21 ± 0.04	0.9 ± 0.2	1.6 ± 0.5	—	1.93 ± 0.1
212.5	0.36 ± 0.04	0.37 ± 0.04	0.27 ± 0.04	0.16 ± 0.03	0.7 ± 0.2	1.4 ± 0.5	0.18 ± 0.08	1.25 ± 0.08
250	0.32 ± 0.04	0.35 ± 0.04	0.25 ± 0.03	0.15 ± 0.03	0.8 ± 0.2	1.7 ± 0.6	0.28 ± 0.12	1.17 ± 0.07
300	0.20 ± 0.03	0.23 ± 0.03	0.18 ± 0.03	0.11 ± 0.02	0.5 ± 0.2	1.1 ± 0.4	0.18 ± 0.06	0.78 ± 0.06
360	0.16 ± 0.02	0.20 ± 0.02	0.16 ± 0.03	0.11 ± 0.02	0.5 ± 0.2	0.5 ± 0.2	0.14 ± 0.06	0.69 ± 0.05

Table 3. Cross sections ${}_{20}\sigma_{0q}$ for two-electron capture in collisions of He^{2+} ions with Cu atoms leading to Cu^{q+} ions for $q = 2$–5. The total two-electron capture cross section σ_{20} is also shown. In addition to the uncertainties shown with individual cross sections, all values are subject to an estimated uncertainty of ±12% in absolute magnitude.

Energy (keV amu^{-1})	${}_{20}\sigma_{02}$ (10^{-17} cm^2)	${}_{20}\sigma_{03}$ (10^{-17} cm^2)	${}_{20}\sigma_{04}$ (10^{-17} cm^2)	${}_{20}\sigma_{05}$ (10^{-17} cm^2)	σ_{20} (10^{-16} cm^2)
35	8.5 ± 1.1	12.2 ± 1.3	3.7 ± 0.5	0.58 ± 0.15	2.50 ± 0.2
40	8.6 ± 1.1	11.4 ± 1.1	3.6 ± 0.4	0.80 ± 0.15	2.44 ± 0.2
46.5	6.5 ± 0.7	8.2 ± 0.9	3.0 ± 0.4	0.67 ± 0.13	1.84 ± 0.1
54	3.7 ± 0.4	4.7 ± 0.5	2.1 ± 0.3	0.46 ± 0.09	1.10 ± 0.1
62.5	2.2 ± 0.2	2.5 ± 0.3	1.11 ± 0.2	0.30 ± 0.06	0.61 ± 0.04
75	1.3 ± 0.14	1.51 ± 0.18	0.68 ± 0.10	0.22 ± 0.04	0.37 ± 0.02
87.5	0.92 ± 0.10	1.02 ± 0.12	0.48 ± 0.07	0.15 ± 0.03	0.26 ± 0.02
105	0.81 ± 0.10	0.95 ± 0.10	0.31 ± 0.05	—	0.21 ± 0.02
125	0.51 ± 0.06	0.58 ± 0.06	0.34 ± 0.06	0.12 ± 0.02	0.16 ± 0.01
150	0.34 ± 0.04	0.40 ± 0.05	0.27 ± 0.05	0.07 ± 0.02	0.11 ± 0.01

Tables 2 and 3 list our measured cross sections ${}_{20}\sigma_{1q}$ and ${}_{20}\sigma_{0q}$ for one- and two-electron capture by He^{2+} ions together with the corresponding total cross sections

$$\sigma_{21} \cong \sum_{q=1}^{q=7} {}_{20}\sigma_{1q} \qquad \text{and} \qquad \sigma_{20} \cong \sum_{q=2}^{q=5} {}_{20}\sigma_{0q}.$$

The uncertainties indicated for individual cross sections reflect 67% confidence levels based on the degree of reproducibility of the measured values. In addition, all cross sections are subject to estimated uncertainties of ±12% in absolute value arising from our normalization procedure.

3.1. One-electron capture by protons

Figure 2 shows measured cross sections ${}_{10}\sigma_{0q}$ for $q = 1$–5 together with total electron capture cross sections σ_{10}. Cross sections ${}_{10}\sigma_{01}$ and ${}_{10}\sigma_{02}$ attain peak values at energies below our low energy limit while there is evidence of maxima in ${}_{10}\sigma_{03}$, ${}_{10}\sigma_{04}$ and ${}_{10}\sigma_{05}$ within the present range. At any particular energy within the present range cross sections decrease with q. It can also be seen that the simple charge transfer cross section ${}_{10}\sigma_{01}$ provides the main contribution to σ_{10} in the energy range considered.

If we consider the outer electron subshell structure $(3s)^2(3p)^6(3d)^{10}$ 4s of copper, it is interesting to consider the likely mechanisms for electron capture. For ${}_{10}\sigma_{01}$ the processes

$$H^+ + Cu \rightarrow H(1s) + Cu^+(4s^{-1}) + 5.9 \text{ eV} \quad (7a)$$

$$\rightarrow H(1s) + Cu^+(3d^{-1}) + 3.4 \text{ eV} \quad (7b)$$

$$\rightarrow H(n = 2) + Cu^+(4s^{-1}) - 4.3 \text{ eV} \quad (7c)$$

$$\rightarrow H(n = 2) + Cu^+(3d^{-1}) - 6.9 \text{ eV} \quad (7d)$$

involving either 4s or 3d electron capture all have small energy defects and might be expected to be important over a wide range of energies including those considered here. The same is true no matter whether Cu^+ product ions are formed in ground or excited states. The process

$$H^+ + Cu \rightarrow H(1s) + Cu^+(3p^{-1}) - 61 \text{ eV} \quad (7e)$$

involving capture of a 3p electron involves a much higher energy defect and might be expected to be relatively less important over most of the present energy range. Indeed, in the absence of momentum transfer to the captured electron, electron capture from a specific subshell might be expected to maximize when $v_T = v + v_p$ where v_T is the orbital velocity of the target electron, v_p is the velocity of the projectile electron in an ion moving with velocity v. In atomic units $v_p = 1$ and v_T can be estimated from $v_T = (Z - S)/n$ where Z is the atomic number of the target, S is the screening parameter of the subshell with principal quantum number n (Fischer 1977). On this basis, 3d and 3p subshell captures might be expected to maximize at proton impact energies of about 200 and 520 keV amu^{-1} respectively. Inspection of our measured cross section curves ${}_{10}\sigma_{0q}$ reveals some evidence of structure around 200 keV amu $^{-1}$ which may reflect 3d capture in addition to 3s capture. However, within the limits of uncertainty shown, there is less evidence for 3p capture around 520 keV amu^{-1}. This may be due in part to the fact that there are only six 3p electrons compared with ten 3d electrons.

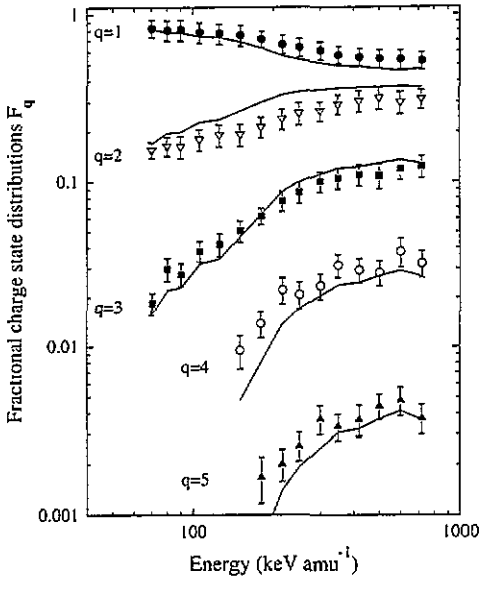

Figure 3. Measured charge state fractions F_q of Cu^{q+} ions (shown by symbols) together with calculated ionization probabilities P_n (full lines) where $n = (q-1)$ based on binomial distribution.

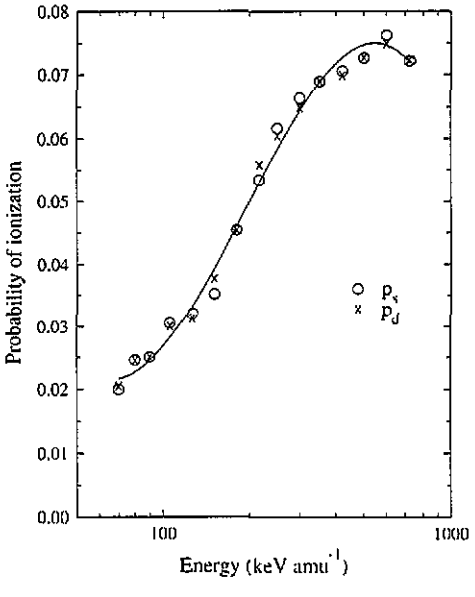

Figure 4. Ionization probabilities p_s and p_d derived from binomial fits to measured charge state distributions.

In the case of transfer ionization cross sections ${}_{10}\sigma_{0q}$ with $q > 1$, electron capture is accompanied by the removal of additional outer electrons the energy for which can be provided through binary-type collisions. Table 4 summarizes the estimated energies required for particular 4s and 3d electron removal mechanisms which would result in ground-state Cu^{q+} ions up to $q = 5$. This treatment is similar to that applied in our recent study of Fe (Patton *et al* 1994).

It is interesting to try to account for the observed relative cross sections for the formation of Cu^{q+} ions. An independent electron description (cf McGuire 1991) is known to be useful in descriptions of multiple ionization. In an attempt to describe the present transfer ionization processes in terms of an independent particle model, we express the probability

Table 4. Energies in eV required for electron removal from Cu to produce Cu^{q+} ions in ground states.

Charge state q	1	2	3	4	5
Energy for removal of last electron (Allen 1973)	7.7	20.3	37.0	58.9	82
Total energy required for removal of outermost electrons in subshells indicated	7.7 $4s^{-1}$	28.0 $4s^{-1}3d^{-1}$	65.0 $4s^{-1}3d^{-2}$	123.9 $4s^{-1}3d^{-3}$	206 $4s^{-1}3d^{-4}$

of one-electron capture and simultaneous ionization as a product of an electron capture probability P_c and an ionization probability P_n for the removal of n electrons from the target where $n \geqslant 0$. In this case $n = (q + 1)$. Then

$$_{10}\sigma_{0q} = 2\pi \int_0^\infty b P_c(b) P_n(b)\, db \tag{8}$$

where b is the impact parameter. If we assume that $P_n(b)$ for ionization is constant over the relatively small range of impact parameters where electron capture occurs then

$$P_n = {}_{10}\sigma_{0q}/\sigma_{10}. \tag{9}$$

The measured fraction F_q of copper ions in a particular charge state q can then be identified with P_n through equation (9).

In the present energy range, one-electron capture is expected to involve either the single 4s electron or one of the ten 3d electrons. If we initially assume that ionization only involves these electrons and that a 3d electron is captured, on the basis of the independent particle model P_n can be expressed as

$$P_n = S_0 D_n + S_1 D_{(n-1)} \tag{10}$$

where S_i and D_j are the respective probabilities of removal of i electrons from the 4s level where $i = 0$ or 1 and j electrons from the 3d level where $j = 0$–9.

Binomial distributions apply if the single ionization probabilities p_s and p_d are the same for an s and d shell respectively in (10) so that $S_i = p_s^i(1 - p_s)^{(1-i)}$ for $i = 0, 1$ and $D_j = \binom{9}{j} p_d^j (1 - p_d)^{(9-j)}$ for $j = 0, 1, 2, \ldots, 9$. Since Cu has only one 4s electron, equation (10) is not complicated by the need to allow for Auger decay if 3d electrons are removed.

Values of P_n predicted by equation (10) have been fitted to the experimentally measured values of F_q obtained from (9) using a weighted least-squares fit. The agreement between experiment and the predictions of the binomial distribution (figure 3) can be seen to be very satisfactory, especially at higher energies where equation (9) becomes increasingly valid as the electron capture cross section (involving smaller impact parameters) decreases.

These fits to the experimental data based on the binomial distribution also provide values of the ionization probabilities p_s and p_d at small impact parameters which are shown in figure 4. The fact that derived values of p_s and p_d are approximately equal provides support for an ionization model based on a structureless cloud (Meron and Rosner 1984). Hence it is unnecessary to specify whether a 4s or a 3d electron has been captured.

It is of some interest to compare the present cross sections $_{10}\sigma_{0q}$ for copper with the corresponding values for iron (Patton *et al* 1994) which has the rather different outer electron subshell structure $(3s)^2(3p)^6(3d)^6(4s)^2$. We have recently used a similar binomial

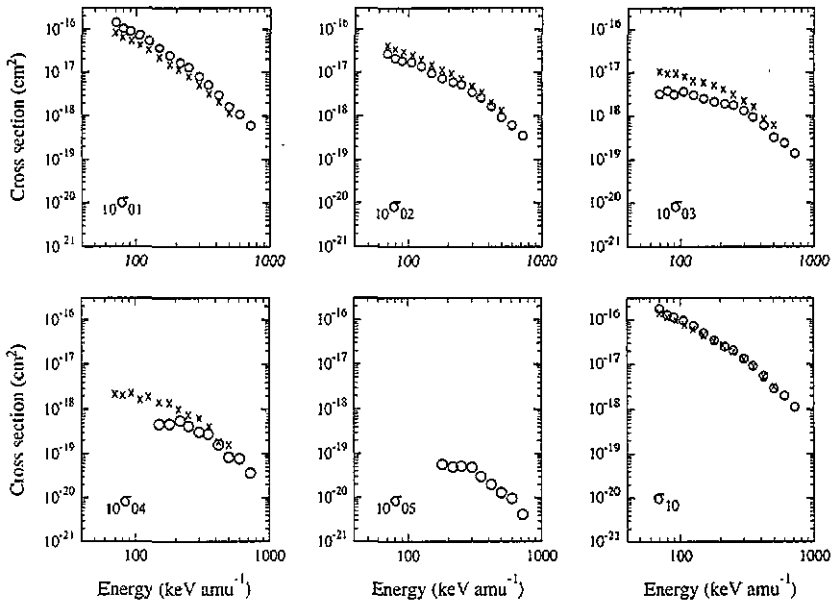

Figure 5. Present cross sections $_{10}\sigma_{0q}$ and σ_{10} for H^+–Cu collisions (shown ○) compared with corresponding values where available for H^+–Fe collisions (shown ×) measured previously by Patton *et al* (1994).

distribution analysis to satisfactorily describe the observed Fe^{q+} product charge distribution in H^+–Fe collisions (Shah *et al* 1995). In addition, total one-electron capture cross sections σ_{10} for iron and copper can be seen (figure 5) to be not greatly different over the full energy range considered. However, simple charge transfer cross sections $_{10}\sigma_{01}$ for copper are a factor of approximately 1.5 times larger than corresponding values for iron. This is close to a ratio of about 1.4 that might be expected as a crude reflection of the total number of 4s and 3d electrons available for capture which is 11 in copper and 8 in iron. In the case of transfer ionization, values of $_{10}\sigma_{02}$, $_{10}\sigma_{03}$ and $_{10}\sigma_{04}$ for iron can be seen to exceed corresponding values for copper, the difference increasing with decreasing energy. These differences are in general qualitative accord with the higher total energies required for the removal of the outermost electrons in copper which are 28, 65 and 124 eV for $q = 2, 3$ and 4 (table 2) compared with 24, 55 and 112 eV respectively in iron (Patton *et al* 1994).

3.2. One- and two-electron capture by He^{2+} ions

Cross sections $_{20}\sigma_{1q}$ for one-electron capture by He^{2+} ions are shown in figure 6. In this case, the transfer ionization cross sections $_{20}\sigma_{12}$ and $_{20}\sigma_{13}$ become as important as simple charge transfer $_{20}\sigma_{11}$ at the highest energies considered. There is also evidence of broad maxima in $_{20}\sigma_{14}$, $_{20}\sigma_{15}$, $_{20}\sigma_{16}$ and $_{20}\sigma_{17}$ within the present group range. The processes

$$He^{2+} + Cu \rightarrow He^+(n = 2) + Cu^+(4s^{-1}) + 6\ eV \qquad (11a)$$

$$\rightarrow He^+(n = 2) + Cu^+(3d^{-1}) + 3\ eV \qquad (11b)$$

$$\rightarrow He^+(1s) + Cu^+(3p^{-1}) - 20\ eV \qquad (11c)$$

all seem likely to contribute to one-electron capture with (11*c*) becoming relatively more important at the highest energies considered. Internal energy considerations in 11(*c*) would

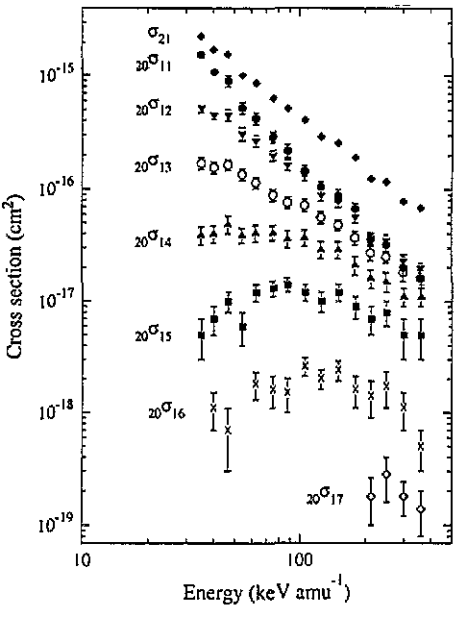

Figure 6. Cross sections $_{20}\sigma_{1q}$ for one-electron capture in collisions of He^{2+} with Cu atoms leading to Cu^{q+} products. Total one-electron capture cross sections σ_{21} are also shown.

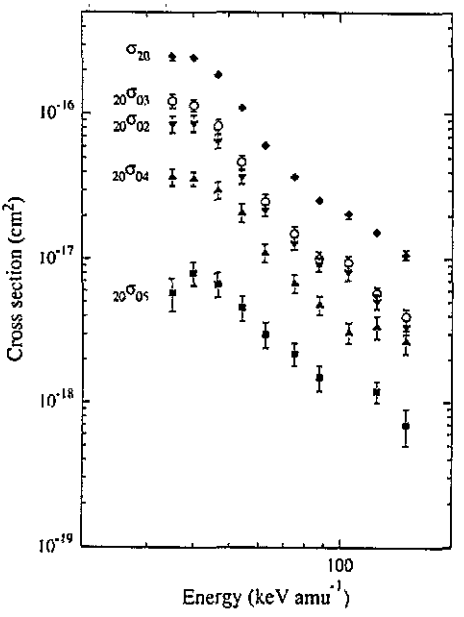

Figure 7. Cross sections $_{20}\sigma_{0q}$ for two-electron capture in collisions of He^{2+} with Cu atoms leading to Cu^{q+} products. Total two-electron capture cross sections σ_{20} are also shown.

allow up to two additional electrons being ejected as a result of Auger transitions. This could explain why $_{20}\sigma_{12}$ and $_{20}\sigma_{13}$ are not greatly different at the highest energies. In addition, we can invoke binary collisions as the mechanism resulting in the ejection of up to six additional electrons. In particular, this mechanism might account for the broad energy dependence observed for $_{20}\sigma_{14}$, $_{20}\sigma_{15}$, $_{20}\sigma_{16}$, and $_{20}\sigma_{17}$.

Cross sections $_{20}\sigma_{0q}$ for two-electron capture by He^{2+} ions are shown in figure 7. In this case simple charge transfer $_{20}\sigma_{02}$ is exceeded by the transfer ionization cross sections $_{20}\sigma_{03}$. In addition $_{20}\sigma_{04}$ becomes comparable with $_{20}\sigma_{03}$ at the highest energies considered. These observations suggest the preference of Auger contributions which depend on which particular electrons undergo electron capture.

As in the case of H^+ impact it is of interest to compare the present cross sections $_{20}\sigma_{1q}$ and $_{20}\sigma_{0q}$ for one- and two-electron capture in He^{2+}–Cu collisions with the corresponding values for He^{2+}–Fe collisions (Patton *et al* 1994). Figure 8 shows the comparison for values of $_{20}\sigma_{1q}$. In the case of the simple one-electron capture cross sections $_{20}\sigma_{11}$ the 'bulge' in the cross section curve for iron in the region of 100 keV amu^{-1} is believed to be due to capture of a 3p electron as in

$$He^{2+} + Fe \rightarrow He^{+}(1s) + Fe^{+}(3p^{-1}) - 10.6\ eV. \tag{12}$$

In copper, where the 'bulge' in the cross section is absent, the corresponding electron capture process would involve an increased energy defect of −20.3 eV so that it is likely to be relatively less important in the present energy range. In addition, electron capture of one of the ten 3d electrons in Cu (compared with six in Fe) seems relatively more likely than electron capture of a 3p electron. It is also interesting to note that, as in the case of H^+ impact, the total electron capture cross sections $_{20}\sigma_{11}$ in Cu exceed corresponding

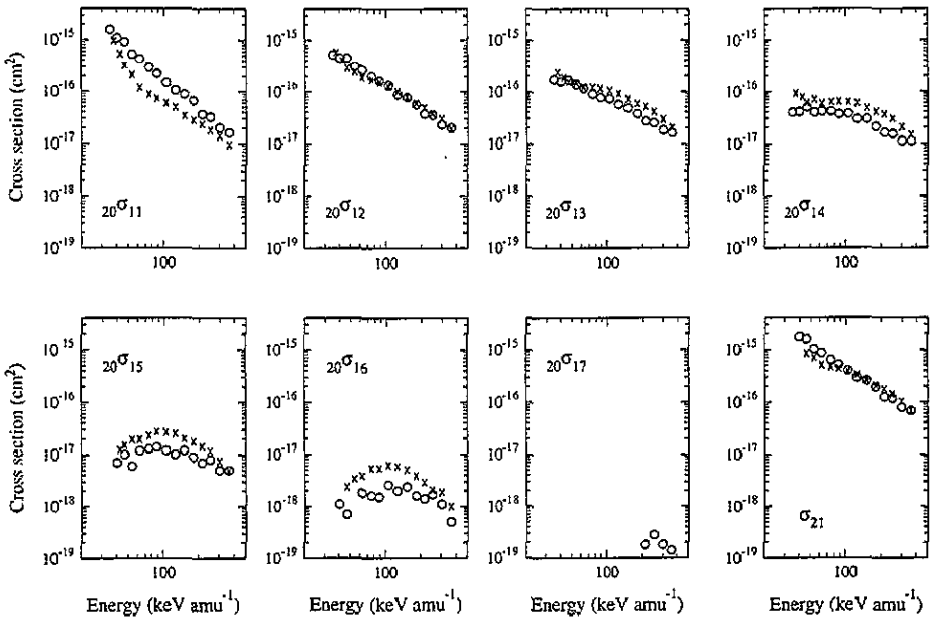

Figure 8. Present cross sections $_{20}\sigma_{1q}$ and σ_{21} for He^{2+}–Cu collisions (shown ○) compared with corresponding values where available for He^{2+}–Fe collisions (shown ×) measured previously by Patton *et al* (1994).

values in iron by a factor which reflects the relative numbers of 3d electrons available. In the case of the transfer ionization cross sections $_{20}\sigma_{1q}$, the energy required for removal of one electron through binary collisions is not greatly different for Cu and Fe. However, less energy is required for removal of additional electrons in Fe. Hence the difference between corresponding values of $_{20}\sigma_{1q}$ generally increases as q increases. We also note that while Auger processes will contribute following 3p capture in both Cu and Fe, the relative differences expected are difficult to assess.

Figure 9 shows the comparison between the two-electron capture cross sections for Cu and Fe. Values of $_{20}\sigma_{0q}$ for Cu can be seen to become increasingly smaller than the corresponding values for Fe as q increases. For $q = 6$, $_{20}\sigma_{0q}$ was too small to measure in Cu. Again, this general trend is consistent with the higher binding energies in Cu as electrons are removed.

4. Conclusions

Transfer ionization in electron capture by H^+ and He^{2+} ions in collisions with Cu atoms has been studied for the first time using a crossed beam coincidence technique. Cross sections $_{10}\sigma_{0q}$ for one-electron capture leading to Cu^{q+} ions in states $q = 1$–5 have been separately determined for impact energies in the range 70–720 keV amu^{-1}. Simple charge transfer (with cross section $_{10}\sigma_{01}$) provides the main contribution to the total one-electron capture cross section in the energy range considered while transfer ionization cross sections $_{10}\sigma_{0q}$ for $q > 1$ decrease with increasing q. An independent electron model has been used to satisfactorily describe the measured fractions of Cu^{q+} ions in states $q = 1$ and $q = 5$ in terms of removal of electrons from the 4s and 3d subshells. Our measured cross sections

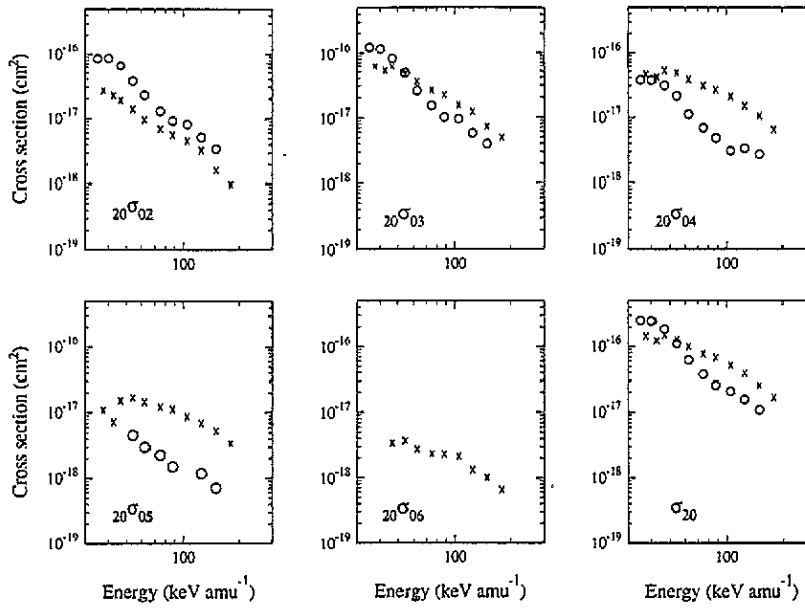

Figure 9. Present cross sections $_{20}\sigma_{0q}$ and σ_{20} for He^{2+}–Cu collisions (shown O) compared with corresponding values where available for He^{2+}–Fe collisions (shown ×) measured previously by Patton *et al* (1994).

$_{20}\sigma_{1q}$ and $_{20}\sigma_{0q}$ for one- and two-electron capture by He^{2+} ions can be considered in terms of electron capture from either 4s, 3d and 3p subshells, together with binary collisions and Auger transitions. Some differences between the present results and our previously measured data for H^+–Fe and He^{2+}–Fe collisions have also been considered in terms of the different electron subshell structures.

Acknowledgments

This research forms part of a programme supported by a Rolling Research Grant from the Engineering and Physical Sciences Research Council. One of us (CJP) is also indebted to the Department of Education, Northern Ireland for the award of a Research Studentship.

References

Allen C W 1973 *Astrophysical Quantities* (London: Athlone) p 36

Bolorizadeh M A, Patton C J, Shah M B and Gilbody H B 1994 *J. Phys. B: At. Mol. Opt. Phys.* **27** 175

Cocke C L and Olson R E 1991 *Phys. Rep.* **205** 153

Fischer C F 1977 *The Hartree–Fock Method for Atoms* (New York: Wiley)

Freund R S, Wetsel R C, Shul R J and Hayes T R 1990 *Phys. Rev.* A **41** 3575

McGuire J H 1991 *Advances in Atomic, Molecular and Optical Physics* vol 29, eds D R Bates and B Bederson (New York: Academic) p 217

Meron M and Rosner B 1984 *Phys. Rev.* A **30** 132

Patton C J, Bolorizadeh M A, Shah M B, Geddes J and Gilbody H B 1994 *J. Phys. B: At. Mol. Opt. Phys.* **27** 3695

Salzborn E and Müller A 1986 *NATO Advanced Studies Institute Series B* vol 145, ed F Brouillard (New York: Plenum) p 357

Shah M B, Elliott D S and Gilbody H B 1987 *J. Phys. B: At. Mol. Phys.* **20** 3051
Shah M B and Gilbody H B 1981 *J. Phys. B: At. Mol. Phys.* **14** 2361
—— 1982 *J. Phys. B: At. Mol. Phys.* **15** 3441
—— 1985 *J. Phys. B: At. Mol. Phys.* **18** 899
Shah M B, McCallion P, Itoh Y and Gilbody H B 1992 *J. Phys. B: At. Mol. Opt. Phys.* **25** 3693
Shah M B, McCallion P, Okuno K and Gilbody H B 1993 *J. Phys. B: At. Mol. Opt. Phys.* **26** 2393
Shah M B, Patton C J, Geddes J and Gilbody H B 1995 *Nucl. Instrum. Methods* B to be published